electronics

Article

Dielectric Resonators Antennas Potential Unleashed by 3D Printing Technology: A Practical Application in the IoT Framework

Francesco Paolo Chietera *, Riccardo Colella and Luca Catarinucci *

Department of Engineering for Innovation, University of Salento, 73100 Lecce, Italy; riccardo.colella@unisalento.it
* Correspondence: francescopaolo.chietera@unisalento.it (F.P.C.); luca.catarinucci@unisalento.it (L.C.)

Abstract: One of the most promising and exciting research fields of the last decade is that of 3D-printed antennas, as proven by the increasing number of related scientific papers. More specifically, the most common and cost-effective 3D printing technologies, which have become more and more widespread in recent years, are particularly suitable for the development of dielectric resonator antennas (DRAs), which are very interesting types of antennas exhibiting good gain, excellent efficiency, and potentially very small size. After a brief survey on how additive manufacturing (AM) can be used in 3D printing of antennas and how much the manufacturing process of DRAs can benefit from those technologies, a specific example, consisting of a wideband antenna operating at 2.4 GHz and 3.8 GHz, was deeply analyzed, realized, and tested. The obtained prototype exhibited compact size ($60 \times 60 \times 16$ mm^3, considering the whole antenna) and a good agreement between measured and simulated S_{11}, with a fractional bandwidth of 46%. Simulated gain and efficiency were also quite good, with values of 5.45 dBi and 6.38 dBi for the gain and 91% and 90% for the efficiency, respectively, at 2.45 GHz and 3.6 GHz.

Keywords: DRA; additive manufacturing; 3D-printed antennas; wideband; IoT; 5G

Citation: Chietera, F.P.; Colella, R.; Catarinucci, L. Dielectric Resonators Antennas Potential Unleashed by 3D Printing Technology: A Practical Application in the IoT Framework. *Electronics* **2022**, *11*, 64. https://doi.org/10.3390/electronics11010064

Academic Editor: Manuel Arrebola

Received: 18 November 2021
Accepted: 22 December 2021
Published: 26 December 2021

1. Introduction

Additive manufacturing (AM) by 3D-printing has increasingly spread in the last decade. This has deeply influenced methods of developing goods in a lot of application fields, allowing greater customization and speeding up the prototyping time of new devices. This is going to be very impactful in the research field for two main reasons. The first is the extremely cost-effective nature of developing prototypes with some common AM technologies, like fused filament fabrication (FFF) and Vat polymerization, including stereolithography (SLS) or digital light processing (DLP). The second reason is that AM allows for the development of devices with unconventional shapes, which could be difficult to manufacture with traditional techniques, thus enabling a lot of new and unexplored applications. These peculiarities make the framework of electromagnetic applications one of the most interesting and fertile fields of research for exploring the use of AM. This interest has been proven by the increasing number of scientific papers published on this topic. An example can be seen in Figure 1, which represents the trend of the term "3D printed antennas" in the last ten years, considering as reference the Google Scholar database. The reported data have been collected by using a python script by Volker Strobel et al. [1].

Specifically, going deeper in analyzing some of the most relevant scientific papers regarding 3D-printed antennas, it emerges how a variety of different devices, designed for different purposes, are realizable with different 3D printing technologies. For example, considering FFF technology, in [2], an RFID reader antenna composed of four planar inverted-F antennas (PIFA) realized onto a substrate with different heights printed using a conventional polylactic acid (PLA) has been described; in [3], the same material was used to realize the substrate of a curved patch antenna, with the metallization obtained using adhesive copper tape; in [4], an acrylonitrile butadiene styrene (ABS) filament has been printed to realize the substrate of a conformal array of antennas, with the conductive parts made by using copper plating technique; in [5], a polycarbonate (PC) filament has been used to print a circular horn antenna with corrugated chokes, which has then been metallized with a conductive silver ink.

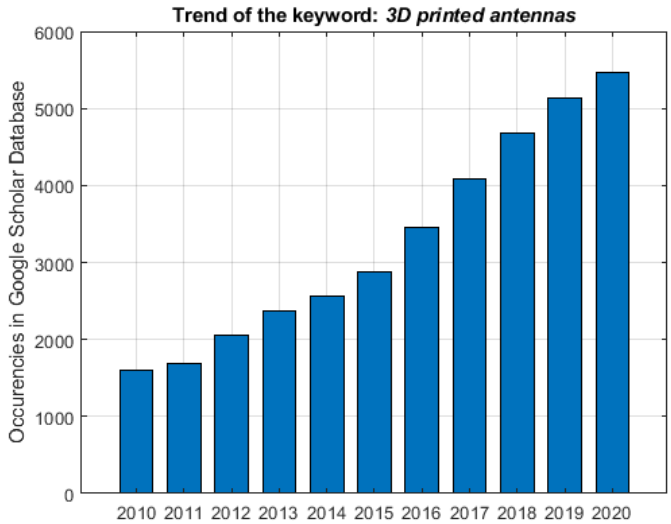

Figure 1. Trend of the term "3D printed antennas" of the last ten years in the Google Scholar database.

As for Vat-polymerization 3D printing technologies, in [6], an interesting hollow structure has been printed with SLA to realize a Yagi-Uda loop antenna utilizing liquid metal to fill the microfluidic channels; in [7], an X-band horn antenna fabricated by an SLA 3D printer in barely 3 h has been described. The metallization has subsequently been obtained by means of a conductive spray coating. In [8], a dual band UHF RFID tag composed by two sliding parts printed using DLP technology has been described and compared with a twin realized with FFF technology.

Conversely, considering technologies with higher setting up costs and more stiff operative constraints, which enable the printing of conductive parts, in [9], both waveguide circuits and antennas realized with binder jetting (BJ) technology, by using metallic powder, have been described, realized, and tested; whilst in [10], direct metal laser sintering (DMLS) technology has been used to realize a wideband conical corrugated horn antenna operating between 25 GHz and 45 GHz.

The aforementioned studies represent only a small part of the many potential applications of 3D printing in electromagnetics that have been explored in the last few years. Many others can be found, for example, in [11], where D. Helena et al. made a great review of the state of the art on 3D printed antennas, by listing and categorizing the applications both for type of technology, material used, and working frequency.

From this preliminary analysis, some considerations can be made on the characteristics of the different techniques. For example, metallic parts are always problematic to create and often need some further manufacturing process to be prototyped. They can be printed, even for high-frequency applications, but using most complex and costly devices (BJ, DMLS, and others that can easily cost thousands of times more than common FFF or SLA/DLP ones). Conversely, the most affordable AM technologies for 3D printing are FFF and Vat-polymerization which, however, only allow users to print polymeric materials. Moreover, most of these commercially available materials exhibit a relatively low dielectric constant (in the range of 2–3). This last factor could be a drawback if it is needed to realize some miniaturized structures or antennas. To overcome this limit, some research on composite materials obtained by combining polymers with some ceramic powders with a high dielectric constant have been carried out. For example, as reported in [12], 3D printing has been used to develop unconventionally shaped molds filled with a flexible silicone rubber/barium titanate ($BaTiO_3$) compound, or in [13,14], where 3D-printable filaments composed of ABS or PLA and barium titanate have been realized, tested, and used to develop electromagnetic applications.

The possibility of easily developing printable high-dielectric-constant devices with unconventional shapes paves the way for the use of 3D printing in developing one specific kind of antenna, which is the dielectric resonator antenna (DRA). These last started to be studied during the early 1980s, when the first paper about a new "Resonant Cylindrical Dielectric Cavity Antenna" was published by Long, McAllister, and Shen [15]. DRAs are particularly suitable for mobile applications due to their small size (depending on the dielectric constant), high efficiency (due to the small amount of metal needed), and, with some shrewdness, wide band. Nevertheless, they are not so common if compared to microstrip antennas because the optimization of the planar manufacturing process better fostered the diffusion of the latter. Conversely, DRAs are traditionally manufactured using subtractive methods and their layouts and costs are particularly influenced by the rigidity of commonly acquirable ceramic parts that are very difficult to be postprocessed. In this regard, these antennas could highly benefit from a production process based on AM. In fact, it could improve their performance, due to the possibility of easily realizing complex shapes, while reducing the costs, which grow with the shape complexity. The impact of these potential advantages on the use of DRAs for a wider and wider range of applications can be summarized by citing Long himself, who recently wrote in one of his last papers [16]: *"The dielectric resonator antenna has to date not seen as many applications as the microstrip antenna; the main obstacle seems to be the higher cost of its more complicated fabrication. However, once new manufacturing techniques such as 3-D printing are further established, and reduced size versions of these radiators for use at very high frequency operations become available, their use is likely to become much more pervasive."*

In the following sections, the main working principles of DRAs will be summarized and the role of AM in overcoming their limits will be discussed. Then, as a proof of concept, a novel design for a compact 3D-printed wideband DRA, operating both in ISM 2.45 GHz and in the 5G-NR band, first proposed in [17], will be realized and tested. The proposed design differs from the previously proposed ones because it aims to exploit multiple aspects at once, as such taking the highest advantage of them. Specifically, a custom lab-made material has been used for the prototype, while in [2–5] commercial materials have been used; An unconventional design to enhance antenna performance, not easily realizable with traditional manufacturing techniques, has been adopted; moreover, the choice of using a DRA for the scope, allowed for the development of the main body of the antenna with a dielectric material, thus avoiding problems related with metallization faced in [5,9,10]. In Table 1, a simplified comparison between the proposed design and the state-of-the-art ones is represented.

Table 1. Comparison among the proposed design and the state-of-the-art ones.

Design	Type of AM Technology and Costs ($)	Use of Customizable High-Dielectric-Constant Material	Use of AM to Realize Unconventional Shape Otherwise Unrealizable	Need for Complex Metallization Procedures
Proposed in this paper	FFF ($)	Yes	Yes	No
Proposed in [2]	FFF ($)	No	No	Yes
Proposed in [3]	FFF ($)	No	Yes	Yes
Proposed in [4]	FFF ($)	No	Yes	Yes
Proposed in [5]	FFF ($)	No	No	Yes
Proposed in [6]	SLA ($$)	No	Yes	Yes
Proposed in [7]	SLA ($$)	No	No	Yes
Proposed in [8]	FFF/DLP ($)	No/Yes	Yes	Yes
Proposed in [9]	BJ ($$$)	No	No	No
Proposed in [10]	DMLS ($$$)	No	Yes	No

2. Dielectric Resonator Antennas Working Principle and Possible Improvements Due to Additive Manufacturing

DRAs are essentially dielectric resonators without metallic enclosures, placed in an open environment in which they can radiate energy when excited by a source. They offer interesting properties, which include:

- Good gain.
- The possibility to realize small-sized antennas because the DRA dimensions are proportional to $\lambda_0/\sqrt{\varepsilon_r}$.
- Excellent efficiency, especially at high frequencies, when compared with metal fabricated antennas, due to the lack of inherent conduction loss inside the dielectric resonators.
- A simple coupling schema that allows users to match DRAs with barely any type of planar transmission line by varying the position of the radiator onto the line.
- The possibility to realize both narrowband as well as wideband and ultrawideband antennas by varying some design parameters.
- The possibility to obtain different radiation characteristics by exciting different modes of a DRA.

These advantages are, however, counterbalanced by two main drawbacks, which are cost and complexity. As for the former, it is typically due to the types of materials and manufacturing processes that are needed to realize a DRA. Indeed, purely ceramic materials, which are traditionally used for the scope, are very difficult to be shaped in complex geometries. Besides, postprocessing, like cutting or drilling holes on them, is very expensive and difficult to realize. As for the latter, the computational complexity grows with the degrees of freedom that can be modified in the final designed structure (e.g., the ratio between the various dimensions of the resonator, the value of ε_r, as well as the type and size of feed).

For both these reasons, the most commonly used geometries in designing DRAs are the three most-known—hemispherical, cylindrical, and rectangular—for which a theoretical analysis has been proposed in [18], by Mongia and Barthia, who gathered the theory of the propagating modes for each of those geometries, giving the equations to predict their resonant frequencies. Over the years, even more complex types of DRAs have been investigated, as reported in the review by Petosa and Ittipiboon [19]. More specifically, low-profile (LP) DRAs have been intensively studied, as well as various methods to tune their working frequency. Different feeding techniques have been analyzed by describing how to obtain linear or circular polarization. Hybrid structures, which are obtained using DRAs to enhance the performance of other types of antennas (e.g., patch antennas), have been explored as well. Eventually, broadband DRAs have been developed, introducing staked or modified geometries—building them with different dielectric constant layers or altering their normal structure by drilling holes on them. Nevertheless, the starting point of all these improvements has always been a common and simple geometry.

In this scenario, the use of AM technologies for the production process represents one of the most promising future research branches, while these kinds of antennas are usually realized by subtractive methods or by simply composing elementary dielectric shapes realized with high-pressure injection or made by firing a green ceramic part. This innovation would lead to more affordable and easily realizable DRAs, making their whole cost comparable with those of planar antennas. Moreover, if the geometric complexity does not influence the production costs anymore, more intricate and unconventional design possibilities, otherwise unrealizable with traditional manufacturing techniques, could be explored to obtain improved results in terms of gain, bandwidth, or radiation pattern.

Obviously, it could be more difficult to handle with arbitrarily complex shapes, at least from a strictly theoretical point of view. Indeed, the analytical approximated formulas that allow for the prediction of working frequency or propagating mode equations are only available for the most common and simple DRA shapes. However, an interesting approach to the problem of analysis and synthesis of unconventional DRAs could be the use of genetic algorithms used to optimize some target functions that can be set up to achieve specific goals. For example, in [20], an interesting approach that exploits a shape generation technique called surface contour shape generation (SCSG), has been described and used to simulate different unconventionally shaped DRAs, comparing their performance. In [21], the so called Gielis' "superformula" has been used as starting point to develop and realize a sub-6GHz 5G DRA using stereolithography with a common commercial resin; eventually, in [22], Gielis himself, together with the other authors, explained how a 3D extension of the superformula could allow researchers to design a very wide range of shapes in an analytical way, and how this capability could be really useful to easily and quickly generate and simulate dielectric lens antennas that fulfill certain constraints.

Once the synthesis of a new DRA shape is completed with one of the previously mentioned methods, the only remaining problem is the individuation of a proper coupling of material and technology suitable for manufacturing the antenna while guaranteeing the dielectric characteristics, in terms of dielectric constant and losses considered during the simulations. Indeed, as stated before, one of the main drawbacks of the polymer-based AM technologies is related to the extremely low dielectric constant that those materials exhibit, which usually ranges between 2 and 3.

With this limitation in mind, and with the support from the colleagues of material engineering of the University of Salento, the authors are developing and characterizing different compound materials, suitable for both FFF and Vat Polymerization, respectively, in the form of ceramic-loaded 3D-printable filaments, and ceramic-loaded photosensitive resins. The goal is to obtain sufficiently low losses, as well as dielectric constant values of around 10, thus filling the last gap that prevents the wider use of the DRA technology empowered by AM. This is a realistic goal, considering that compound materials have dielectric properties that are a compromise between those of their two phases. Besides, overcoming that value too much could lead to a very high quality factor of the resulting DRA that would determine a very narrow band, which is not always desirable.

In the following section, a new and unconventional design for a wideband DRA, operating between 2.4 and 3.8 GHz (covering WiFi/Bluetooth as well as 5G-NR band) has been simulated, realized, and measured. The manufacturing process has been carried out using FFF technology, exploiting one of the mentioned prototypal materials to realize the main component of the resonating structure. Specifically, the material chosen for the scope was a PLA-based filament enhanced with barium titanate at 17.5% in volume, exhibiting a dielectric constant of 5 and a loss tangent of 0.015. Those values have been measured using a lab-made T-resonator, realized by some of the authors and described in [23], to measure the characteristics of a $100 \times 100 \times 2$ mm^3 substrate printed with a standard FFF printer and a 100% infill.

3. Design of an Unconventionally Shaped Wideband DRA for IoT Communications

The process of designing the antenna has been carried out with two goals in mind. The first was to obtain a DRA exhibiting a wideband behavior that allowed it to be suitable for IoT communications. For this reason, the operating frequency range was chosen to be between 2.4 GHz and 3.8 GHz, thus enabling applications in both the ISM band and in the forthcoming 5G sub-6 GHz band. The second goal was to miniaturize the overall structure as much as possible while preserving good radiating performance.

In order to match these needs, a complex design composed by two rectangular elements of increasing size, stacked up one on the other, has been studied as a base to achieve a wideband behavior. Indeed, it is well known how this kind of DRA composed of different substrates can fulfill this purpose [24]. Moreover, to achieve a LP DRA design, while enlarging the bandwidth, the technique of using a metallic top load onto the upper part of the resonator was adopted, as suggested in [19,25]. Finally, a rounded fillet has been applied to the edges at the center of the resonator, in order to increase the gain and slightly increase the bandwidth, by smoothing the transition of the electromagnetic field from one element to the other of the stack.

A comparison between the simulated S_{11} curves of the three previously discussed designs—the one with two stacked elements, the one with the addition of the metallic top load, and the final one with the further addition of the rounded fillet to the central edges—is shown in Figure 2.

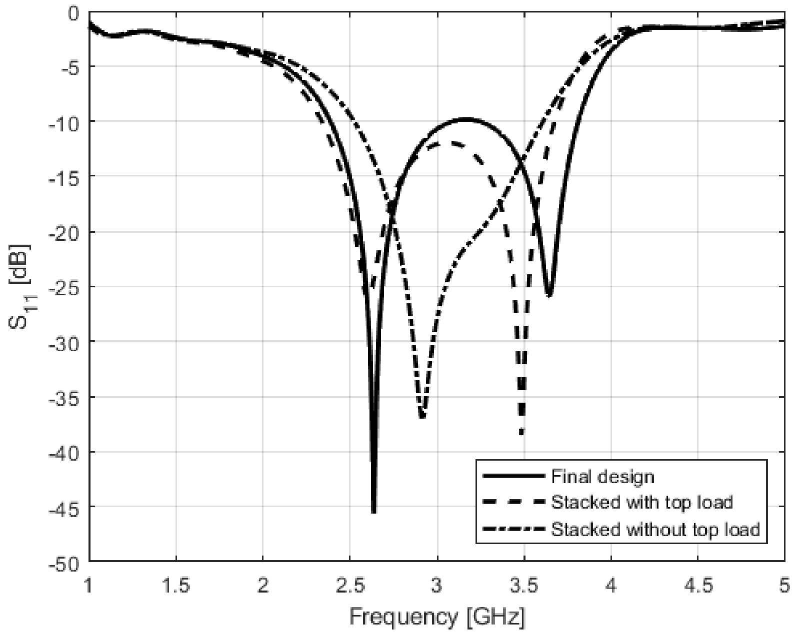

Figure 2. Trend of the keyword "3D printed antennas" occurrences of the last ten years in the Google Scholar database.

As for the feeding method, a microstrip feed slot has been centered at the bottom of the dielectric resonator. This technique was chosen both to easily excite the TE^{Z}_{111} mode in the resonator, so producing a field oriented in the normal direction of the antenna main surface, as well as for easiness of fabrication. Its dimensions are 37×6 mm^2, while the distance between the end of the microstrip and the nearest edge of the slot is 8 mm. If we consider the slot without the DR on top of it, it exhibits a good S_{11} matching at both 4.1 GHz and 6.3 GHz.

Due to the complexity of the antenna design, an accurate analytical analysis of the resonant frequencies was not possible, so a deep simulation campaign has been carried out to optimize it, using the full-wave software CST Microwave Studio. A graphical overview of the final design can be observed in Figure 3, where both a rendered view of the antenna as well as a technical drawing reporting all the tuned dimensions are depicted. As can be seen, the rectangular elements of the DRA have been considered to have a square base, so as to simplify the optimization procedure by maintaining the ratio between the base sides as constant and equal to 1. Moreover, the low profile is achieved with a ratio between the height and the maximum width of the DRA, which resulted as 1:4.

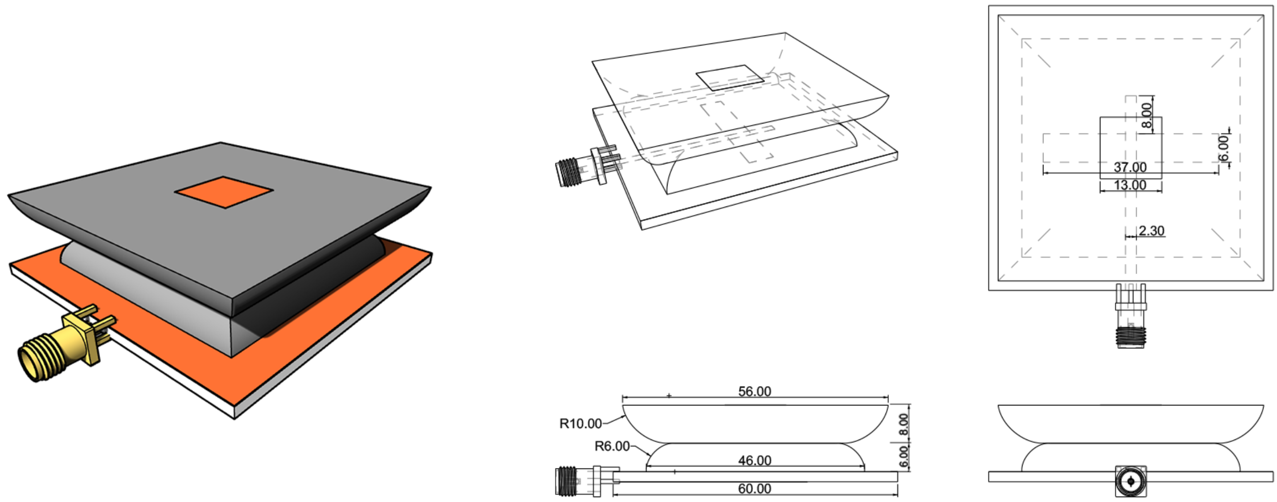

Figure 3. Rendered view of the DRA (on the **left**). Technical views of the DRA with dimensions in mm (on the **right**).

4. Realization and Measurements

As stated, the FFF technology has been used to realize the main element of the DRA by using a lab-made printable filament with enhanced dielectric properties. It has been printed with a Prusa MINI+ desktop 3D printer [26], using the printing settings listed in Table 2.

Table 2. Printing settings used for the PLA-$BaTiO_3$ (17.5% Vol.) filament.

Extrusion Temperature	Bed Temperature	Infill	Speed
210 °C	60 °C	100%	60 mm/s

Conversely, for the substrate hosting the microstrip feed slot, it has been realized by using a commercial PREPERM PPE1200 substrate of 60 × 60 × 2 mm^3 [27], while the metallic parts have been shaped onto a copper adhesive tape, through a Graphtec CE 6000-40 cutting plotter [28]. Some pictures of the realized prototype can be seen in Figure 4, where both the resonator and the microstrip feed slotted substrate are shown before and after the assembling procedure. The two elements have been locked together by means of a very thin layer of silicone glue.

The so-realized device has been measured by using a Siglent SVA1075X Vector Network Analyzer (VNA) and calibrated with a Siglent F604FS kit to determine the S_{11} curve. The comparison between measured and simulated results is shown in Figure 5, where a picture taken during the measurements is also reported. As can be seen, there was a very good agreement between simulations and measurements, and the overall bandwidth of the realized prototype exhibited values even larger than the simulated ones, which led to a fractional bandwidth (FB) slightly less than 46%.

The maximum gains for both 2.45 GHz and 3.6 GHz (which are the center frequencies of the two band of interest) were 5.45 dBi for the former and 6.38 dBi for the latter, as can be seen in Figure 6, where the co-polarized and cross-polarized gain radiation patterns are shown in both E-plane and H-plane. For the former (Figure 6a), the main lobe directions were $-3°$ and $+3°$ for the two frequencies, while the 3 dB angular width was 98.8° at 2.45 GHz and 73.4° at 3.6 GHz, respectively. For the latter (Figure 6b), the main lobe directions were 0° for the two frequencies, while the 3 dB angular width was 94.3° at 2.45 GHz and 75° at 3.6 GHz, respectively. The low value of cross-polarization indicates, as expected, that the prototyped antenna was linearly polarized. For an easier visualization, the 3D versions of the antenna radiation gain patterns, are shown in Figure 7, as well as the maximum gain and the values of total and radiation efficiency over frequency.

These values can allow researchers to calculate an interesting metric that can easily give an idea of the miniaturization goodness achieved by the antenna prototype. This is the so-called miniaturized antenna figure of merit (MAFM), which was defined in [29] by the equation:

$$\mathrm{MAFM_{dB}} = 10\log_{10}\left(\eta \cdot \frac{\Delta f}{f_c} \cdot \frac{\lambda}{D}\right), \quad (1)$$

where η is the antenna efficiency; $\Delta f / f$ is the FB; λ is the free-space wavelength, and D is the largest linear dimension of the antenna. The proposed prototype exhibited a $\mathrm{MAFM}^{2.45\mathrm{GHz}} = -0.053$ dB if evaluated at 2.45 GHz and a $\mathrm{MAFM}^{3.6\mathrm{GHz}} = -2.56$ dB if evaluated at 3.6 GHz, which are quite good results if it is considered that a simple half-wavelength dipole with a 99% efficiency and a narrow band of 5% has a MAFM of about -10.04 dB.

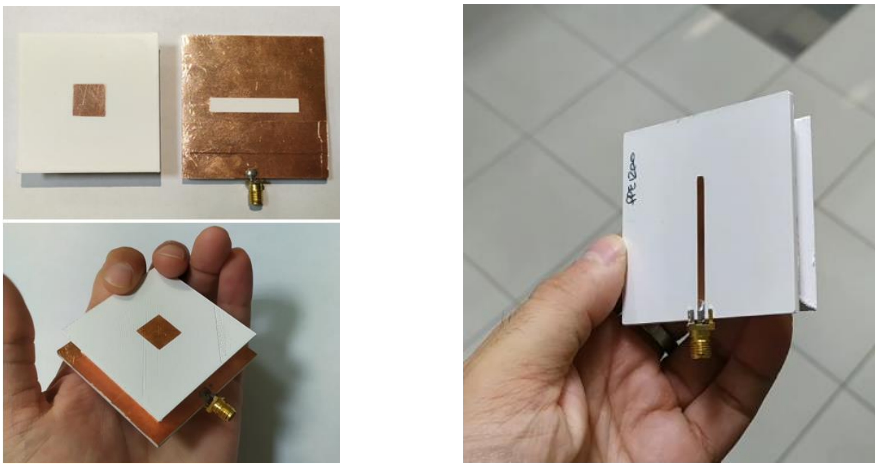

Figure 4. Top view of both the resonator element and the slotted ground plane disassembled (on **top left corner**). Top frontal views of the assembled DRA (on **bottom left corner**). Bottom view of the assembled DRA (on the right).

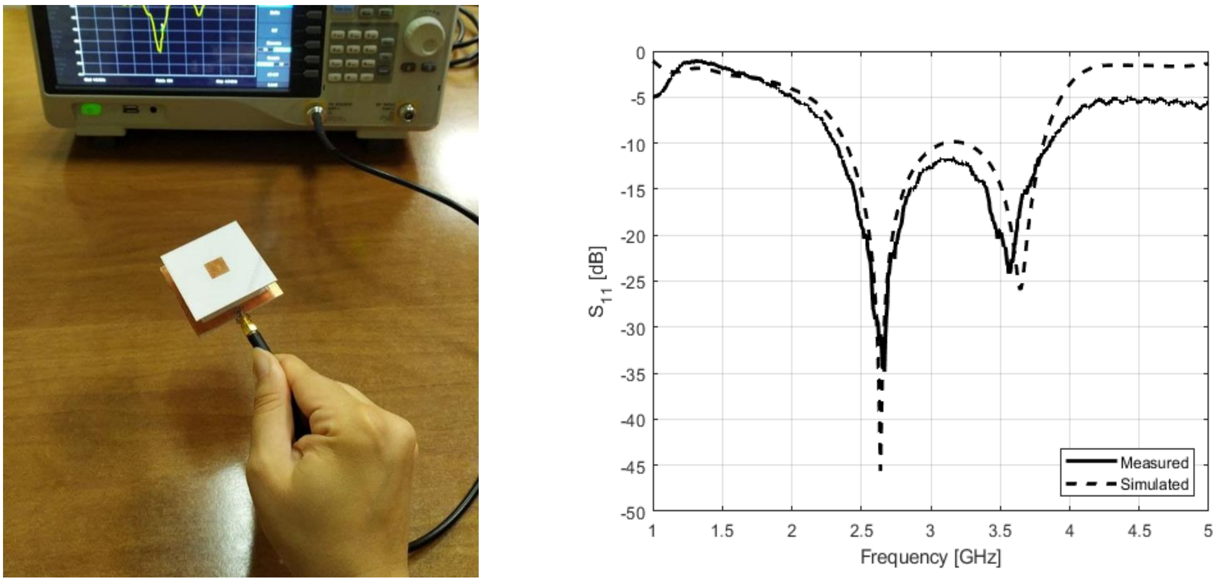

Figure 5. Picture of the measurement procedure (on the **left**). Comparison of the measured and simulated S_{11} curves (on the **right**).

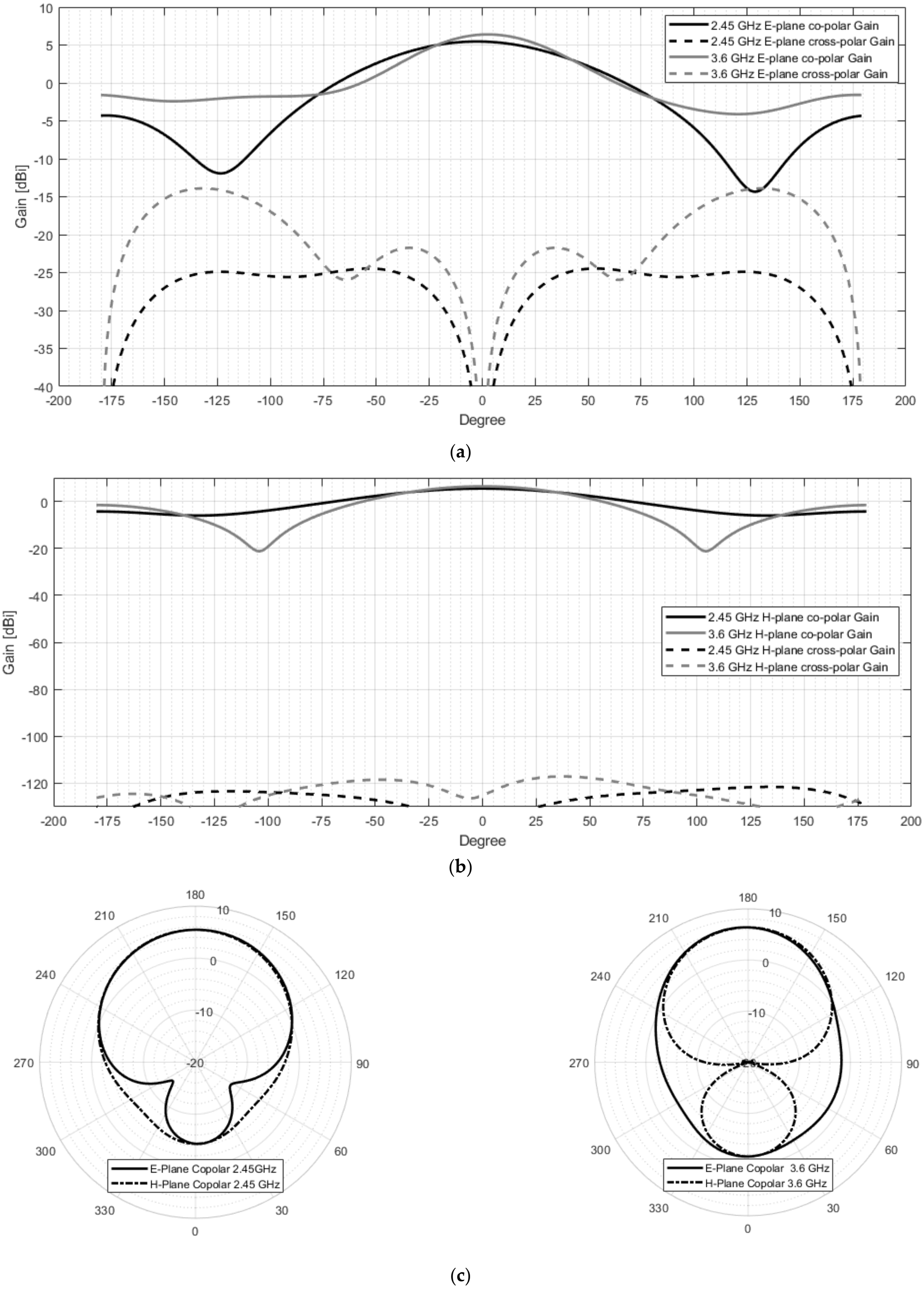

Figure 6. Simulated co-polarized and cross-polarized gain radiation pattern in the E-plane (**a**) and H-plane (**b**) for the cartesian form, and in polar form (**c**), for the two main working frequencies.

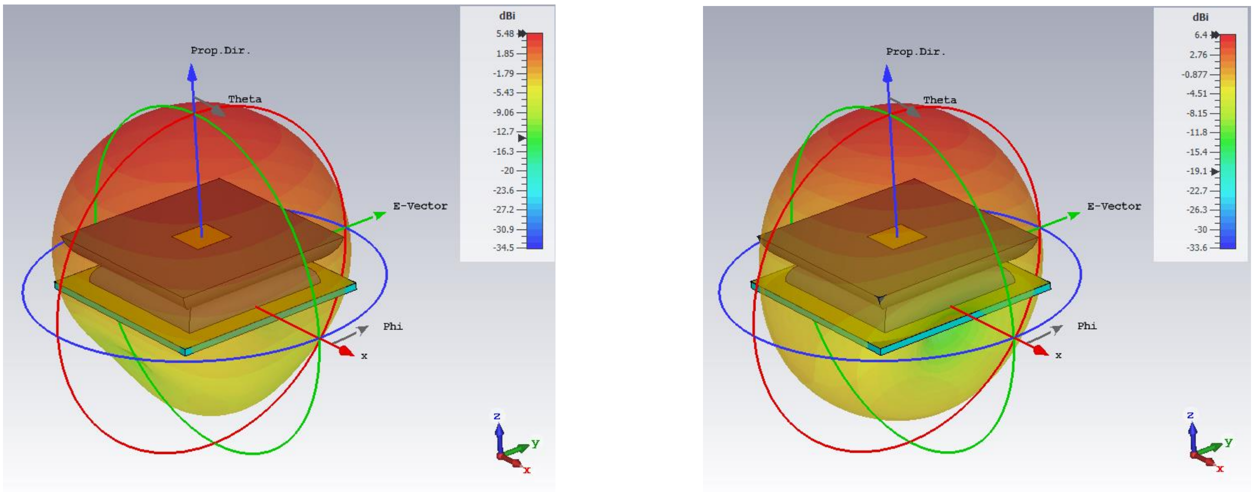

(**a**)

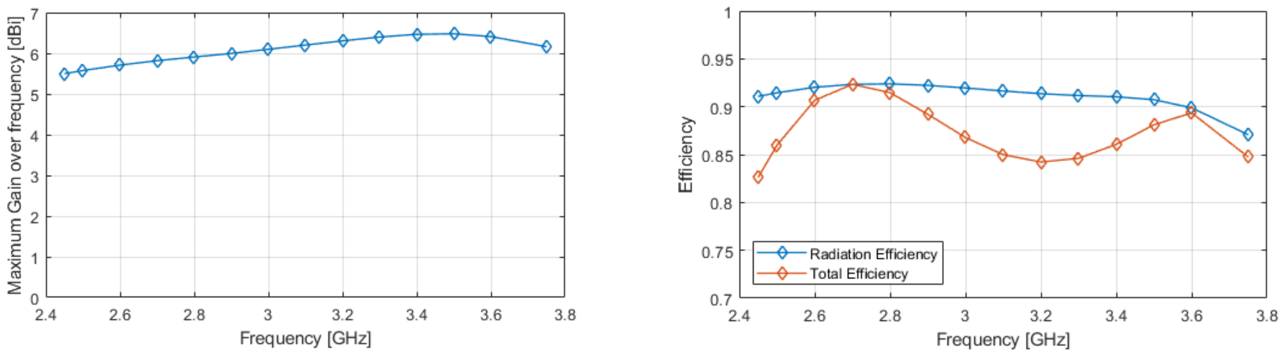

(**b**)

Figure 7. 3D views of the antenna gain radiation patterns (**a**) for both 2.45 GHz and 3.6 GHz. Maximum gain (left), and efficiencies (right) plots (**b**) over frequency.

5. Conclusions

In this work, a brief analysis of the state of the art on the matter of "3D printed antennas" was carried out, highlighting how different AM technologies can be suitable for applications with different constraints. The problem of prototyping conductive parts emerged to be one of the most challenging aspects in developing a manufacturing process for fully 3D-printed antennas. In this scenario, DRAs, with their inherent dielectric nature and their great degree of freedom in choosing the antenna shape, seem to be the most promising type of antennas to overcome the problem, while taking advantage of the use of AM. In this regard, the various improvements that AM can lead to in the realization of new, unconventional, and cost-effective DRAs have been discussed and a practical application consisting of a wideband antenna operating between 2.4 GHz and 3.8 GHz has been described. Specifically, the designed and simulated antenna protype has been realized using the FFF technology empowered by a lab-made PLA/$BaTiO_3$ material to reach the project constraints. The performance of the developed device has been subsequently evaluated and the measurements emerged to be in good agreement with simulations, thus proving the potential of AM technologies in realizing DRAs.

Author Contributions: Conceptualization, F.P.C., R.C. and L.C.; methodology, L.C.; investigation, F.P.C.; writing—original draft preparation, F.P.C.; writing—review and editing, R.C. and L.C.; visualization, F.P.C.; supervision, L.C.; project administration, L.C. All authors have read and agreed to the published version of the manuscript.

Funding: This research received no external funding.

Institutional Review Board Statement: Not applicable.

Informed Consent Statement: Not applicable.

Data Availability Statement: For any data supporting results presented in this paper, please contact Luca Catarinucci at luca.catarinucci@unisalento.it.

Conflicts of Interest: The authors declare no conflict of interest.

References

1. Strobel, V. *Pold87/Academic-Keyword-Occurrence: First Release (V1.0.0)*; Zenodo, 2018. Available online: https://doi.org/10.5281/zenodo.1218409 (accessed on 18 November 2021).
2. Colella, R.; Catarinucci, L.; Michel, A.; Nepa, P. Design of a 3D-printed circularly polarized antenna for portable UHF RFID readers. In Proceedings of the 2017 IEEE International Conference on RFID Technology & Application (RFID-TA), Warsaw, Poland, 20–22 September 2017; pp. 225–228.
3. Muntoni, G.; Montisci, G.; Casula, G.A.; Chietera, F.P.; Michel, A.; Colella, R.; Catarinucci, L.; Mazzarella, G. A Curved 3-D Printed Microstrip Patch Antenna Layout for Bandwidth Enhancement and Size Reduction. *IEEE Antennas Wirel. Propag. Lett.* **2020**, *19*, 1118–1122. [CrossRef]
4. Fenn, A.J.; Pippin, D.J.; Lamb, C.M.; Willwerth, F.G.; Aumann, H.M.; Doane, J.P. 3D printed conformal array antenna: Simulations and measurements. In Proceedings of the 2016 IEEE International Symposium on Phased Array Systems and Technology (PAST), Waltham, MA, USA, 18–21 October 2016; pp. 1–4.
5. Castro, A.T.; Sharma, S.K. A triple mode waveguide corrugated horn antenna using 3D printing technology. In Proceedings of the 2017 IEEE International Symposium on Antennas and Propagation & USNC/URSI National Radio Science Meeting, San Diego, CA, USA, 9–14 July 2017; pp. 1235–1236.
6. Adeyeye, A.O.; Bahr, R.A.; Tentzeris, M.M. 3D Printed 2.45 GHz Yagi-Uda Loop Antenna Utilizing Microfluidic Channels and Liquid Metal. In Proceedings of the 2019 IEEE International Symposium on Antennas and Propagation and USNC-URSI Radio Science Meeting, Atlanta, GA, USA, 7–12 July 2019; pp. 1983–1984.
7. Zhu, X.; Zhang, B. A Low-Cost Stereolithography Printed X-band Antenna with Metallic-Plated Surface. In Proceedings of the 2019 International Conference on Microwave and Millimeter Wave Technology (ICMMT), Guangzhou, China, 19–22 May 2019; pp. 1–3.
8. Colella, R.; Chietera, F.P.; Catarinucci, L. Analysis of FDM and DLP 3D-Printing Technologies to Prototype Electromagnetic Devices for RFID Applications. *Sensors* **2021**, *21*, 897. [CrossRef] [PubMed]
9. Purushothama, J.M.; Lopez-Soriano, S.; Vena, A.; Sorli, B.; Susanti, I.; Perret, E. Electronically Rewritable Chipless RFID Tags Fabricated Through Thermal Transfer Printing on Flexible PET Substrates. *IEEE Trans. Antennas Propag.* **2021**, *69*, 1908–1921. [CrossRef]
10. Wu, L.; Wang, C.; Peng, S.; Guo, Y. 3-D Printed Wideband Millimeter-Wave Horn Antenna with Conical Radiation Pattern. *IEEE Antennas Wirel. Propag. Lett.* **2020**, *19*, 453–456. [CrossRef]
11. Helena, D.; Ramos, A.; Varum, T.; Matos, J.N. Antenna Design Using Modern Additive Manufacturing Technology: A Review. *IEEE Access* **2020**, *8*, 177064–177083. [CrossRef]
12. Catarinucci, L.; Chietera, F.P.; Colella, R. Permittivity-Customizable Ceramic-Doped Silicone Substrates Shaped With 3-D-Printed Molds to Design Flexible and Conformal Antennas. *IEEE Trans. Antennas Propag.* **2020**, *68*, 4967–4972. [CrossRef]
13. Khatri, B.; Lappe, K.; Habedank, M.; Mueller, T.; Megnin, C.; Hanemann, T. Fused Deposition Modeling of ABS-Barium Titanate Composites: A Simple Route towards Tailored Dielectric Devices. *Polymers* **2018**, *10*, 666. [CrossRef] [PubMed]
14. Colella, R.; Chietera, F.P.; Montagna, F.; Greco, A.; Catarinucci, L. Customizing 3D-Printing for Electromagnetics to Design Enhanced RFID Antennas. *IEEE J. Radio Freq. Identif.* **2020**, *4*, 452–460. [CrossRef]
15. McAllister, M.W.; Long, S.A. Rectangular Dielectric Resonator Antenna. *IEE Electron. Lett.* **1983**, *19*, 218–219. [CrossRef]
16. Jackson, D.R.; Long, S.A. History of Microstrip and Dielectric Resonator Antennas. In Proceedings of the 2020 14th European Conference on Antennas and Propagation (EuCAP), Copenhagen, Denmark, 15–20 March 2020; pp. 1–5.
17. Chietera, F.P.; Colella, R.; Catarinucci, L. The Promising Role of 3D-printed Dielectric Resonator Antennas in the IoT Framework. In Proceedings of the 2021 6th International Conference on Smart and Sustainable Technologies (SpliTech), Bol and Split, Croatia, 8–11 September 2021; pp. 1–4. [CrossRef]
18. Mongia, R.K.; Bhartia, P. Dielectric resonator antennas—A review and general design relations for resonant frequency and bandwidth. *Int. J. Microw. Millim. Wave Comput. Aided Eng.* **1994**, *4*, 230–247. [CrossRef]
19. Petosa, A.; Ittipiboon, A. Dielectric Resonator Antennas: A Historical Review and the Current State of the Art. *IEEE Antennas Propag. Mag.* **2010**, *52*, 91–116. [CrossRef]
20. Whiting, E.B.; Campbell, S.D.; Mackertich-Sengerdy, G.; Werner, D.H. Dielectric Resonator Antenna Geometry-Dependent Performance Tradeoffs. *IEEE Open J. Antennas Propag.* **2021**, *2*, 14–21. [CrossRef]
21. Basile, V.; Grande, M.; Marrocco, V.; Laneve, D.; Petrignani, S.; Prudenzano, F.; Fassi, I. Design and Manufacturing of Super-Shaped Dielectric Resonator Antennas for 5G Applications Using Stereolithography. *IEEE Access* **2020**, *8*, 82929–82937. [CrossRef]

22. Mescia, L.; Bia, P.; Caratelli, D.; Chiapperino, M.A.; Stukach, O.; Gielis, J. Electromagnetic Mathematical Modeling of 3D Supershaped Dielectric Lens Antennas. *Math. Probl. Eng.* **2016**, *2016*, 8130160. [CrossRef]
23. Catarinucci, L.; Colella, R.; Coppola, P.; Tarricone, L. Microwave characterisation of polylactic acid for 3D-printed dielectrically controlled substrates. *IET Microw. Antennas Propag.* **2017**, *11*, 1970–1976. [CrossRef]
24. Keyrouz, S.; Caratelli, D. Dielectric Resonator Antennas: Basic Concepts, Design Guidelines, and Recent Developments at Millimeter-Wave Frequencies. *Int. J. Antennas Propag.* **2016**, *2016*, 6075680. [CrossRef]
25. Luk, K.M.; Leung, K.W. *Dielectric Resonator Antennas*; Research Studies Press: Baldock, UK, 2003.
26. Prusa MINI+ 3D Printer. Available online: https://shop.prusa3d.com/it/stampanti-3d-/994-original-prusa-mini.html (accessed on 22 October 2021).
27. PREPERM PPE1200 60 × 60 × 2. Available online: https://www.preperm.com/webshop/product/preperm-ppe1200-2x60x60-plaque/ (accessed on 22 October 2021).
28. Graphtec CE6000 Series Cutting Plotter. Available online: https://www.graphtec-italia.it/prodotti/graphtec-ce6000/ (accessed on 22 October 2021).
29. Buerkle, A.; Sarabandi, K.; Mosallaei, H. Compact slot and dielectric resonator antenna with dual-resonance, broadband characteristics. *IEEE Trans. Antennas Propag.* **2005**, *53*, 1020–1027. [CrossRef]